

## Molecular dynamics-derived conformation and intramolecular interaction analysis of the *N*-acetyl-9-*O*-acetylneuraminic acid-containing ganglioside G<sub>D1a</sub> and NMR-based analysis of its binding to a human polyclonal immunoglobulin G fraction with selectivity for *O*-acetylated sialic acids

Hans-Christian Siebert, Claus-Wilhelm von der Lieth<sup>1</sup>,  
Xin Dong, Gerd Reuter, Roland Schauer, Hans-Joachim  
Gabius and Johannes F.G. Vliegthart<sup>3,4</sup>

Institut für Physiologische Chemie, Tierärztliche Fakultät,  
Ludwig-Maximilians-Universität, Veterinärstraße 13, D-80539 München,  
Germany, <sup>1</sup>Deutsches Krebsforschungszentrum, Zentrale Spektroskopie, Im  
Neuenheimer Feld 280, D-69120 Heidelberg, Germany, <sup>2</sup>Biochemisches  
Institut, Christian-Albrechts-Universität, Olshausenstraße 40, D-24098 Kiel,  
Germany, and <sup>3</sup>Bijvoet Center for Biomolecular Research, Utrecht  
University, P.O. Box 80075, NL-3508 TB Utrecht, The Netherlands

<sup>4</sup>To whom correspondence should be addressed

The influence of 9-*O*-acetylation of G<sub>D1a</sub>, yielding G<sub>D1a</sub> (<sup>6</sup>Neu5,9Ac<sub>2</sub>) with a 9-*O*-acetylated sialic acid moiety linked to the outer galactose residue, on the spatial extension and mobility of the carbohydrate chain and on recognition by a natural human antibody is analysed. To study a potential impact of the *O*-acetyl group on the overall conformation of the carbohydrate chain, molecular dynamics (MD) simulations of oligosaccharide chain fragments of increasing length starting from the non-reducing end have been carried out for the first time in this study. They revealed a considerable loss in chain flexibility after addition of the internal *N*-acetylneuraminic acid onto the chain. Besides MD calculations with different dielectric constants, the conformational behaviour of the complete oligosaccharide chain of the 9-*O*-acetylated G<sub>D1a</sub> ganglioside was simulated in the solvents water and dimethyl sulfoxide. These solvents were also used in NMR measurements. The results of this study indicate that 9-*O*-acetylation at the terminal sialic acid does not influence the overall conformation of the ganglioside. An extended interaction analysis of energetically minimized conformations of G<sub>D1a</sub> (<sup>6</sup>Neu5,9Ac<sub>2</sub>) and G<sub>D1a</sub>, obtained during molecular dynamics simulations, allowed assessment of the influence of the different parts of the saccharide chains on spatial flexibility. Noteworthy energetic interactions, most interestingly between the 9-*O*-acetyl group and the pyranose ring of *N*-acetylgalactosamine, were ascertained by the calculations. However, the strength of this interaction does not force the ganglioside into a conformation, where the 9-*O*-acetyl group is no longer accessible. Binding of G<sub>D1a</sub> (<sup>6</sup>Neu5,9Ac<sub>2</sub>) to proteins, which are specific for 9-*O*-acetylated sialic acids, should thus at least partially be mediated by the presence of this group. To experimentally prove this assumption, a NMR study of 9-*O*-acetylated G<sub>D1a</sub> in the presence of an affinity-purified polyclonal IgG fraction from human serum with preferential binding to 9-*O*-acetylated sialic acid was performed. The almost complete disappearance of the intensity of the 9-*O*-acetyl methyl signal of the G<sub>D1a</sub> (<sup>6</sup>Neu5,9Ac<sub>2</sub>) clearly indicates that the assumed interaction of the 9-*O*-acetyl group with the human protein takes place.

*Key words:* sialic acid/ganglioside/molecular dynamics/  
conformation/NMR/antibody

Gangliosides are sialic acid-containing glycosphingolipids that are ubiquitous components of the mammalian plasma membrane. They are assumed to play important roles in the interaction of cells with their environment, and are apparently involved in the regulation of many cellular events (Hakomori, 1990, 1991; Kopitz, 1996). Since the carbohydrate part of naturally occurring gangliosides can be modified, e.g., by 9-*O*-acetylation of sialic acids (Reuter and Schauer, 1987), the presence of such alterations prompts evaluation of their structural impact on conformation and molecular recognition. Following this reasoning, we have focused in the present study on G<sub>D1a</sub> and its 9-*O*-acetylated derivative G<sub>D1a</sub> (<sup>6</sup>Neu5,9Ac<sub>2</sub>) carrying the *N*-acetyl-9-*O*-acetylneuraminic acid exclusively linked to the terminal galactose moiety of the tetrasaccharide backbone Galβ1–3GalNAcβ1–4Galβ1–4Glc, whereas the internal galactose residue is substituted by *N*-acetylneuraminic acid (Gowda *et al.*, 1984). A schematic representation of the oligosaccharide part of G<sub>D1a</sub> (<sup>6</sup>Neu5,9Ac<sub>2</sub>), denoted as fragment IV in the text, is shown in Figure 1.

In relation to the knowledge about the occurrence of *O*-acetylated gangliosides, relatively little is known concerning the functions of this modification. A major impact of *O*-acetylation of sialic acids may be the protection against the action of sialidases (Schauer, 1979, 1982; Varki, 1992), which initiate the catabolism of these compounds. In addition, 9-*O*-acetylation is considered a differentiation marker in developmental processes (Varki, 1992; Klein *et al.*, 1994; Schauer *et al.*, 1995) or, e.g., in the form of the gangliosides G<sub>D3</sub> (<sup>6</sup>Neu5,9Ac<sub>2</sub>) and G<sub>D2</sub> (<sup>6</sup>Neu5,9Ac<sub>2</sub>), as tumour-associated antigens in human melanomas (Cheresh *et al.*, 1984a,b; Thurin *et al.*, 1985; Ravindranath *et al.*, 1988; Manzi *et al.*, 1990; Sjöberg *et al.*, 1992). Owing to the rather high level of expression of G<sub>D3</sub> (<sup>6</sup>Neu5,9Ac<sub>2</sub>) in melanomas, attempts to turn this feature into therapeutic benefit have been initiated (Ravindranath *et al.*, 1989; Ritter *et al.*, 1989, 1990). Turning from tumours to viral infections, sialic acid *O*-acetylation can mediate or prevent receptor binding, as shown for viral adhesion. Whereas it reduces the extent of binding of the pathogenic influenza A-virus strain, the adhesins of the C-type virus and the coronavirus exhibit a high affinity to this modified sialic acid residue (Herrler *et al.*, 1985; Zimmer *et al.*, 1992, 1994; Schultze *et al.*, 1993). Masking of ligand recognition by 9-*O*-acetylation is not restricted to pathogens, as substantiated by the lack of binding of the B-cell adhesion molecule CD22b to the modified sialic acid (Sjöberg *et al.*, 1994). It has also recently been shown that the 9-*O*-acetyl group of Neu5,9Ac<sub>2</sub> interferes with sialoadhesin binding (Kelm *et al.*, 1994). In this

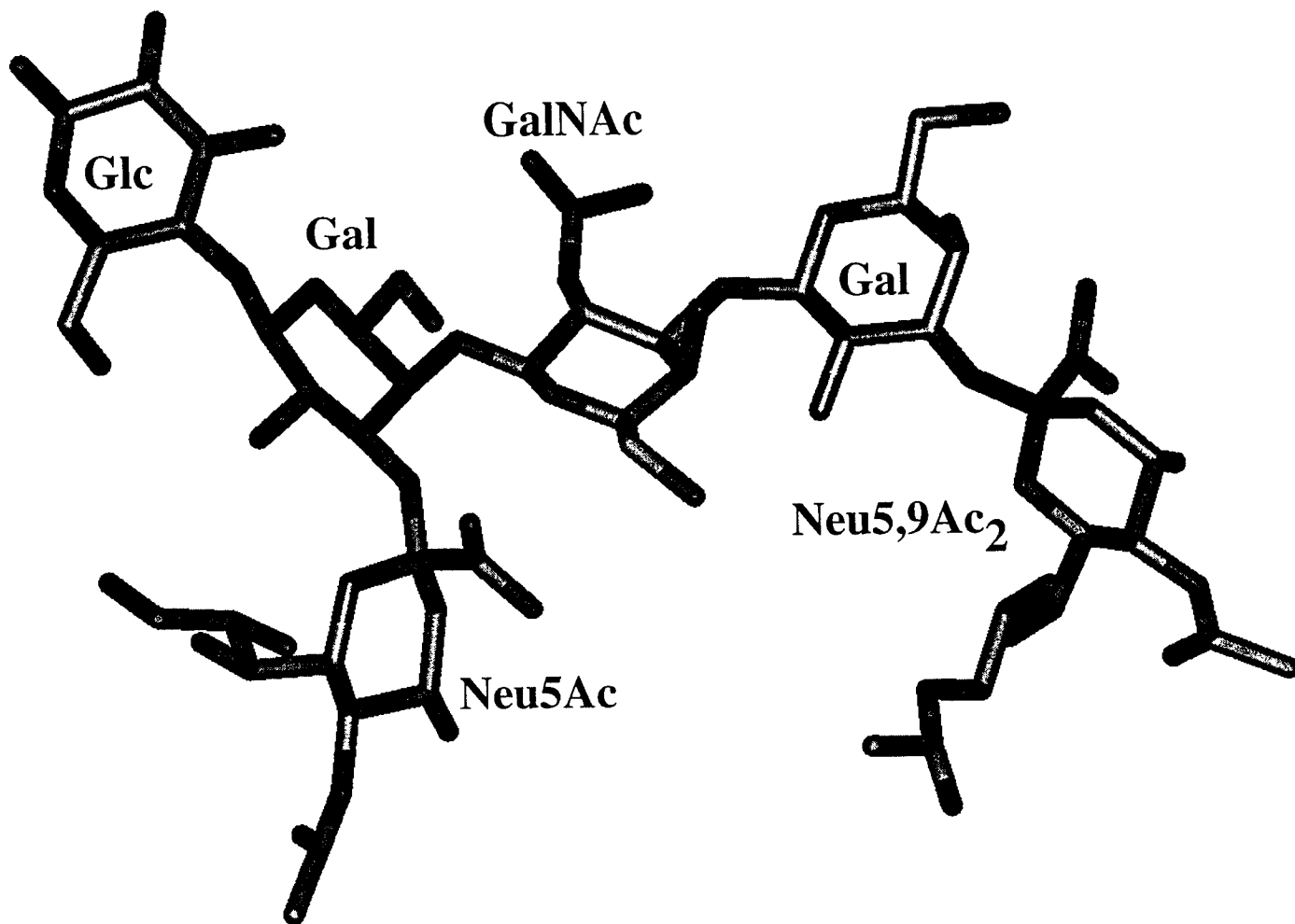


Fig. 1. Schematic representation of the oligosaccharide part of  $G_{D1a}$  ( $^c\text{Neu5,9Ac}_2$ ) (fragment IV).

context the presence of a polyclonal antibody fraction in human serum with apparent specificity for 9-*O*-acetylated sialic acids is intriguing (Ahmed and Gabius, 1989; Zeng and Gabius, 1992). The expression of specific binding proteins in serum supports the notions that *O*-acetylation can be a marker for recognitive events by proteins and that the presence of such markers in certain tumour types may serve as target for the binding of natural antibodies and for attempts of active immunisation. However, detailed information about the recognition mechanism of *O*-acetyl groups on a molecular level is important to understand their biological role(s). Therefore, we used  $G_{D1a}$  and  $G_{D1a}$  ( $^c\text{Neu5,9Ac}_2$ ) in the present study as proper models to contribute to the evaluation of the specific role(s) of *O*-acetylation of sialic acids in complex glycoconjugates.

## Results and discussion

For this study CVFF was selected because it is a well established force field, describing the conformational behaviour of  $\text{GM}_3$ -gangliosides in good agreement with the NMR data (Siebert *et al.*, 1992). During the parametrization and validation of CVFF (Hagler *et al.*, 1974, 1979a,b), emphasis has also been put on the description of intermolecular forces, especially OH-bonds in small charged molecules. Thus, the bifunctionality of the OH-group (hydrogen bond donor as well as hydrogen

bond acceptor) is included in the parametrization. This is a basic feature important for carbohydrates. Calculated structural parameters such as bond lengths and bond angles are comparable to other force fields used to describe carbohydrate properties. It should be pointed out that CVFF does not contain—as many other force fields do—any special parametrization or term to describe the anomeric and/or exoanomeric effect. Good agreement between experimental and theoretical results for model oligosaccharides using CVFF to explore the conformational space has been reported during the last few years (Balaji *et al.*, 1992, 1994; Siebert *et al.*, 1992, 1996a,b; Asensio *et al.*, 1995; von der Lieth *et al.*, 1996), although the force field is not able to reproduce consistently the correct vibrational frequency, which is an indication for possible limitations of accuracy of the force field (Homans *et al.*, 1990; Marti *et al.*, 1994). Nonetheless, it has proven useful to process binding data of oligosaccharide ligands for the asialoglycoprotein receptor (Balaji *et al.*, 1993) and the conformational behaviour of high-mannose oligosaccharides (Balaji *et al.*, 1994). To further substantiate our choice of the force field, we refer to a study where NMR data of  $\alpha$ -lactoside have been compared with the results of molecular dynamics (MD)-simulations using the CVFF, CVFF91, AMBER, and AMBER/Homans parametrization (Asensio *et al.*, 1995). It was found that the conformational behaviour predicted by CVFF is closer to the experi-

mental results, as for example the one resulting from AMBER/Homans parametrization. In the same line of reasoning the conformational space of maltose has been explored using different force fields (CVFF, CVFF91, AMBER, AMBER/Homans, MM+) (Kozár, 1995). In accordance with Asensio *et al.* (1995), the results obtained by the use of CVFF reach the predictive quality of the other force fields.

*MD-derived conformations of fragments and of the complete oligosaccharide chain of G<sub>D1a</sub> (<sup>e</sup>Neu5,9Ac<sub>2</sub>)*

NMR-derived, energetically minimized molecular mechanics (MM) conformations of fragments of the carbohydrate chain of G<sub>D1a</sub> (<sup>e</sup>Neu5,9Ac<sub>2</sub>) with an increasing length starting from the non-reducing terminus of the oligosaccharide chain were used as input data for 1000 ps MD simulations at 300 K to study the influence of non-bonded interactions on the conformation of the complete molecule. The corresponding NMR data that are available from the literature (Scarsdale *et al.*, 1990; Sabesan *et al.*, 1991a,b; Acquotti *et al.*, 1994; Poppe *et al.*, 1994) were obtained for the non-*O*-acetylated G<sub>D1a</sub> and proved to be helpful for comparing this study with our own results (Siebert, 1990) that already included NMR measurements of the 9-*O*-acetylated derivative G<sub>D1a</sub> (<sup>e</sup>Neu5,9Ac<sub>2</sub>).

The following oligosaccharide parts of G<sub>D1a</sub> (<sup>e</sup>Neu5,9Ac<sub>2</sub>) were generated and then separately analysed as detailed in *Materials and methods*:

- (I): <sup>e</sup>Neu5,9Ac<sub>2</sub>α2-3Galβ1-3GalNAc;  
 (II): <sup>e</sup>Neu5,9Ac<sub>2</sub>α2-3Galβ1-3GalNAcβ1-4Gal;  
 (III): <sup>e</sup>Neu5,9Ac<sub>2</sub>α2-3Galβ1-3GalNAcβ1-4(<sup>i</sup>Neu5Acα2-3)Gal; and  
 (IV): <sup>e</sup>Neu5,9Ac<sub>2</sub>α2-3Galβ1-3GalNAcβ1-4(<sup>i</sup>Neu5Acα2-3)Galβ1-4Glc.

The <sup>e</sup>Neu5,9Ac<sub>2</sub>α2-3Gal linkage in fragments I and II shows transitions between two distinct conformations as can be deduced from the two sets of  $\Phi$ ,  $\Psi$  angles of this linkage (Figure 2a). This conformational behaviour is similar to that determined by MD simulations for Neu5Acα2-3Gal linkages in G<sub>M3</sub> gangliosides (Siebert *et al.*, 1992) and in oligosaccharide chain fragments of glycoproteins (Siebert *et al.*, 1993). The flexibility of the <sup>e</sup>Neu5,9Ac<sub>2</sub>α2-3Gal linkage is reduced in fragment III, in which a second sialic acid (<sup>i</sup>Neu5Ac) is linked α-glycosidically to the 3 position of the internal galactose. This change can be recognized from the data in Figure 2a, where only one pair of  $\Phi$ ,  $\Psi$  values can be deduced with confidence from the MD calculations, and from the  $\Phi$ ,  $\Psi$  trajectories, given in Figure 3, that clearly indicate a higher flexibility of the <sup>e</sup>Neu5,9Ac<sub>2</sub>α2-3Gal in fragment II than in fragment III. A further extension of fragment III to fragment IV, which represents the complete oligosaccharide chain of G<sub>D1a</sub> (<sup>e</sup>Neu5,9Ac<sub>2</sub>), does not seem to alter significantly the conformation with respect to fragment III (Figure 2a).

In addition, the orientations of both sialic acid glycerol side chains are given for fragment IV, revealing an appreciable flexibility of both side chains as indicated by the corresponding values of  $\omega_8$  and  $\omega_9$ , respectively (Figure 2b,c). A similar degree of flexibility of the sialic acid side chain(s) was also calculated for shorter fragments (I–III) of the oligosaccharide. These results yield further refined information about the existence of distinct conformers depending on the oligosaccharide chain length on the basis of previous literature data about G<sub>D1a</sub> (Acquotti *et al.*, 1994). To address the argument that the monitored simulation time of 1000 ps at 300 K could be too short to

a)

fragment I	$\Phi$ (SD)	$\Psi$ (SD)
Neu5,9Ac <sub>2</sub> α2-3Gal	-80 (13)	-20 (10)
	-160 (12)	-22 (14)
Galβ1-3GalNAc	33 (30)	-17 (19)
fragment II	$\Phi$ (SD)	$\Psi$ (SD)
Neu5,9Ac <sub>2</sub> α2-3Gal	-81 (19)	7 (14)
	-165 (13)	-19 (10)
Galβ1-3GalNAc	27 (29)	-15 (19)
GalNAcβ1-4Gal	-131 (35)	14 (13)
fragment III	$\Phi$ (SD)	$\Psi$ (SD)
<sup>e</sup> Neu5,9Ac <sub>2</sub> α2-3Gal	-97 (18)	19 (13)
Galβ1-3GalNAc	-25 (21)	-21 (11)
GalNAcβ1-4Gal	32 (9)	16 (10)
<sup>i</sup> Neu5Acα2-3Gal	-165 (11)	-15 (9)
fragment IV	$\Phi$ (SD)	$\Psi$ (SD)
<sup>e</sup> Neu5,9Ac <sub>2</sub> α2-3Gal	-96 (27)	27 (13)
Galβ1-3GalNAc	-22 (23)	-24 (10)
GalNAcβ1-4Gal	36 (10)	15 (10)
<sup>i</sup> Neu5Acα2-3Gal	-170 (9)	-20 (9)
Galβ1-4Glc	39 (27)	-8 (18)

b)

$\omega_6$ (SD)	$\omega_7$ (SD)	$\omega_8$ (SD)	$\omega_9$ (SD)	$\omega_{10}$ (SD)
-65 (9)	180 (10)	50 (15)	180 (19)	180 (14)
		70 (13)	85 (15)	
			-80 (18)	

c)

$\omega_6$ (SD)	$\omega_7$ (SD)	$\omega_8$ (SD)
-65 (9)	180 (23)	50 (17)
		-55 (19)

**Fig. 2.** MD calculations of the  $\Phi$ ,  $\Psi$  angles of the glycosidic linkages within the four carbohydrate fragments of G<sub>D1a</sub> (<sup>e</sup>Neu5,9Ac<sub>2</sub>) (a) and of the torsion angles  $\omega_6 - \omega_{10}$  of the exocyclic side chains of (<sup>e</sup>Neu5,9Ac<sub>2</sub>) (b) and of (<sup>i</sup>Neu5Ac) (c) of fragment IV; SD, standard deviation.

register the range of additional conformational changes, a temperature increase to 400 K was included into the simulation (Sun and Kollman, 1992). No significant changes with regard to the values obtained for 300 K and shown here were detected.

A major drawback of MD calculations in vacuum is the explicit exclusion of solvent molecules that can easily be expected to influence the conformation. This problem can in the first step be addressed by simulation of the solvent in performing the calculations with dielectric constants  $\epsilon \geq 1$ . Application of  $\epsilon$  values of 4 and 80, the latter simulating water, to the calculations of G<sub>D1a</sub> (<sup>e</sup>Neu5,9Ac<sub>2</sub>) did not result in appearance of different conformations.

*MD simulations of G<sub>D1a</sub> (<sup>e</sup>Neu5,9Ac<sub>2</sub>) with explicit inclusion of water and DMSO*

MD simulations with application of suitable dielectric constants  $\epsilon$  as well as with the tedious and time-consuming calculations with the inclusion of the actual solvent molecules are practically feasible due to the availability of adequate computer programs. Thus, corresponding calculations for G<sub>D1a</sub> (<sup>e</sup>Neu5,9Ac<sub>2</sub>) over a time period of 150 ps have been carried out in water and DMSO, both of which have also been used as solvents for the NMR experiments of this ganglioside, and for G<sub>D1a</sub>. Although the inclusion of solvent or as a box with periodic boundary conditions leads to a more accurate description of the oligosaccharide dynamics than obtained with simulations at certain  $\epsilon$  values, the computational calculations become extremely time-consuming for larger molecules. For proteins it has been reported that good agreement with the crystal

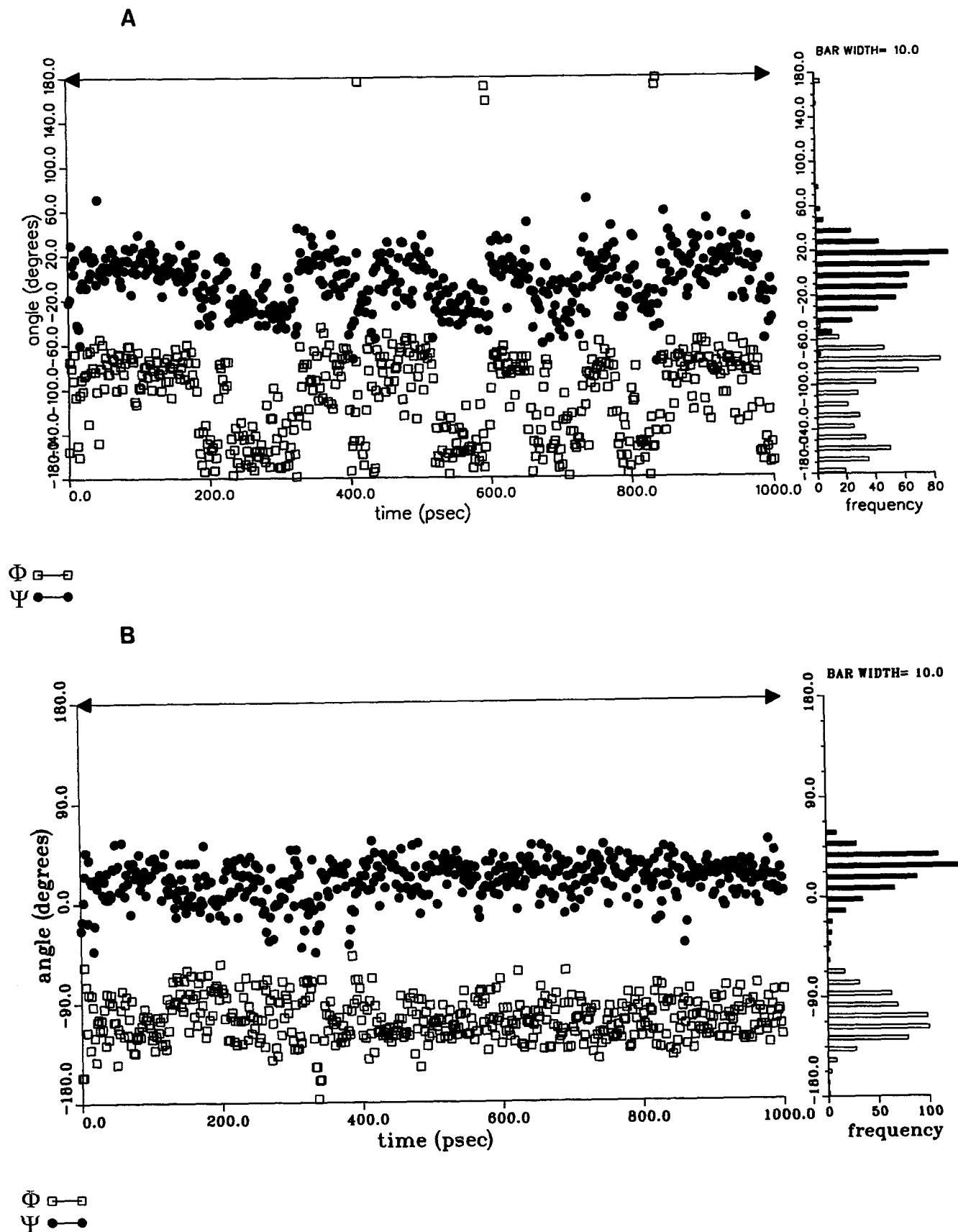


**Fig. 3.** Conformational behaviour of oligosaccharide fragments of the carbohydrate chain of the ganglioside. The trajectories of a 1000 ps MD simulation of  $G_{D1a}$  ( $^c\text{Neu5,9Ac}_2$ ) at 300 K and  $\epsilon = 80$  represent the time-dependent alteration of the glycosidic angles  $\Phi$  and  $\Psi$  of the Neu5,9Ac<sub>2</sub>- $\alpha$ -2-Gal-linkage of either fragment II (A) or fragment III (B).

structure can be achieved when a single hydration sphere and a distance-dependent dielectric constant were used (Guenet and Kollman, 1992, 1993). Consequently, it appears credible to simulate with this assumption and then extend to as much solvent water as is computationally feasible. The results of MD simulations are described in Figure 4, where the  $\Phi$ ,  $\Psi$  angles obtained for the glycosidic linkages of fragment IV are given for  $G_{D1a}$  ( $^e\text{Neu5,9Ac}_2$ ) in a water box with periodic boundary conditions (Figure 4a), in a water layer (Figure 4b), and in a DMSO box with periodic boundary conditions (Figure 4c). In the case of the periodic boundary conditions, the integration step had to be reduced to 0.125 fs, because local overheating effects will otherwise cause ring inversions, which mainly occur for the GalNAc-residue, whereas calculations with the water layer did not give ring-inversion or evaporation under these conditions. All these simulations of  $G_{D1a}$  ( $^e\text{Neu5,9Ac}_2$ ) yielded similar results independent of the nature of the solvent, which corroborate the data obtained by MD simulations of  $G_{D1a}$  ( $^e\text{Neu5,9Ac}_2$ ) with no explicit inclusion of water molecules at dielectric constants  $\epsilon$  of 4 or 80. The only difference that appears to be significant is exhibited in the Gal $\beta$ 1-4Glc linkage within fragment IV. It may adopt various  $\Phi$ ,  $\Psi$  angles depending on the type of the solvent and the solvation sphere, underscoring its remarkable flexibility already displayed in simulations with deliberate alterations of the  $\epsilon$ -value without explicit consideration of solvent molecules.

#### Interaction analysis of $G_{D1a}$ ( $^e\text{Neu5,9Ac}_2$ )

The apparently tremendous influence of the inner *N*-acetylneuraminic acid ( $^e\text{Neu5Ac}$ ) on the conformation and flexibility of the complete oligosaccharide chain of  $G_{D1a}$  ( $^e\text{Neu5,9Ac}_2$ ) (fragment IV) clearly indicates that interactions

between different, spatially separated parts of  $G_{D1a}$  ( $^e\text{Neu5,9Ac}_2$ ) can exist. Thus, an interaction analysis of the constituents of  $G_{D1a}$  ( $^e\text{Neu5,9Ac}_2$ ) and, for comparison,  $G_{D1a}$  will probably allow comprehension of the relevance of individual influences. Likewise, the impact of the presence of the 9-*O*-acetyl group can be studied in this kind of analysis. The MD simulations of energetically minimized  $G_{D1a}$  ( $^e\text{Neu5,9Ac}_2$ ) and  $G_{D1a}$  served as a basis for the interaction analysis. For this aim, the complete oligosaccharide chains of the two gangliosides were treated as composed of 15 different structural units A–O (Figure 5). Energy values describing these interactions are listed in Figure 6. These data result from a simulation at 300 K using a dielectric constant of  $\epsilon = 4$  after 500 and 1000 ps of simulation time. The van der Waals energy values can be calculated by subtracting the Coulomb energy values from the total energy values. Total energy values exceeding about  $\pm 2$  kcal/mol are considered to be indicative of an interaction of different structural units. The indicated simulations allow deduction of contacts of distant monosaccharide residues that are not observable by NMR measurements, i.e., interactions between the *N*-acetyl substituent of the outer sialic acid moiety with the pyranose ring of the inner *N*-acetylneuraminic acid (C–M) and, in the context of these studies most interestingly, between the 9-*O*-acetyl group of the outer sialic acid unit and the pyranose ring of *N*-acetylgalactosamine (A–H). Since the interactions H–J and C–M are not dependent on 9-*O*-acetylation, they are also seen in the case of  $G_{D1a}$ , whereas the contact A–H is only present in  $G_{D1a}$  ( $^e\text{Neu5,9Ac}_2$ ). Its absolute energy value is rather low ( $-4.22$  kcal/mol) after 1000 ps simulation. However, it is significantly less favourable after 500 ps ( $-1.19$  kcal/mol) than after 1000 ps. The intermediate energy values obtained at the various 50 ps intervals over the whole simulation period of 1000 ps show the same differences as given here exemplarily for 500 and 1000 ps rather than a steady decrease to  $-4.22$  kcal/mol. This result is consistent with the notion that the interaction seen, e.g., after 1000 ps simulation can exist within one conformational arrangement, but is not strong enough to arrest the whole oligosaccharide chain in a corresponding conformation. It has to be noted that the same results that are not detectable by direct NOE contacts due to the distances of appropriate protons of more than 4 Å were obtained with MD simulations using different dielectric constants  $\epsilon$  as well as under explicit consideration of the presence of solvent molecules.

#### Conformational aspects of $G_{D1a}$ ( $^e\text{Neu5,9Ac}_2$ )

On the basis of NMR spectroscopic data and computational calculations, the establishment of a hydrogen bonding network between the external and the internal sialic acid, which may influence the overall conformation of  $G_{D1a}$ , has been discussed (Scarsdale *et al.*, 1990; Sabesan *et al.*, 1991a; Acquotti *et al.*, 1994; Poppe *et al.*, 1994). Consequently, the introduction of a 9-*O*-acetyl group may weaken this hydrogen bonding network between the two sialic acid moieties, leading to a completely different conformation or dynamic behaviour. The present data notably extend available information about  $G_{D1a}$  in explicitly including solvent molecules in the calculation and in performing interaction analyses. In addition, a detailed conformational and dynamic analysis of  $G_{D1a}$  ( $^e\text{Neu5,9Ac}_2$ ) is given here for the first time. It is obvious that the conformational impacts described in the literature for  $G_{D1a}$  are confirmed herein. 9-*O*-Acetylation of the outer sialic acid apparently does not lead to

a)			
fragment IV	$\Phi$ (SD)	$\Psi$ (SD)	
$^e\text{Neu5,9Ac}_2\alpha 2-3\text{Gal}$	-75 (20)	-10 (15)	
Gal $\beta$ 1-3GalNAc	-30 (22)	-40 (11)	
GalNAc $\beta$ 1-4Gal	30 (23)	15 (13)	
$^i\text{Neu5Ac}\alpha 2-3\text{Gal}$	-175 (18)	-35 (14)	
Gal $\beta$ 1-4Glc	60 (27)	-30 (16)	

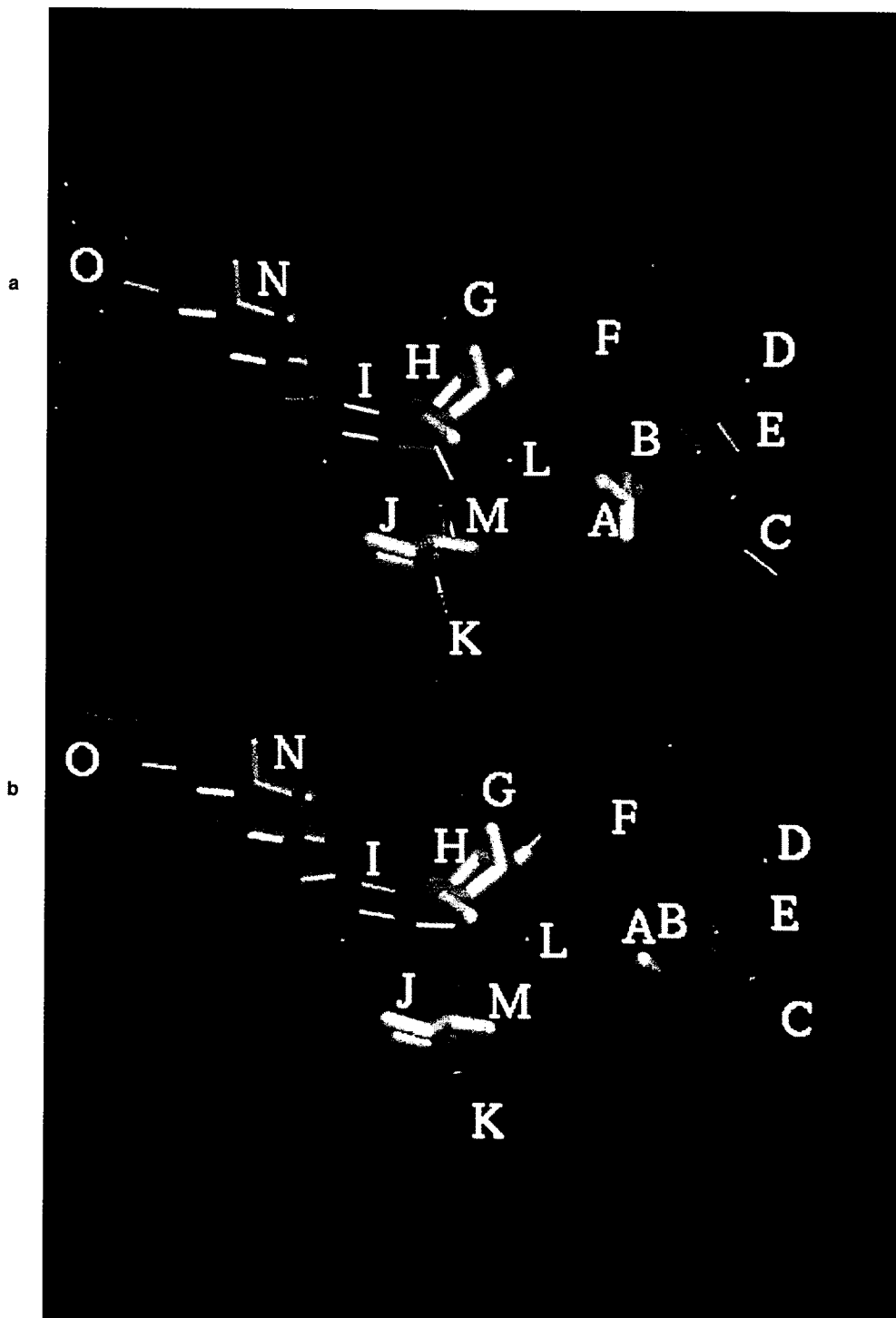
  

b)			
fragment IV	$\Phi$ (SD)	$\Psi$ (SD)	
$^e\text{Neu5,9Ac}_2\alpha 2-3\text{Gal}$	-90 (23)	20 (13)	
Gal $\beta$ 1-3GalNAc	-50 (18)	-20 (14)	
GalNAc $\beta$ 1-4Gal	20 (19)	20 (14)	
$^i\text{Neu5Ac}\alpha 2-3\text{Gal}$	-175 (16)	-15 (12)	
Gal $\beta$ 1-4Glc	120 (32)	-30 (17)	

c)			
fragment IV	$\Phi$ (SD)	$\Psi$ (SD)	
$^e\text{Neu5,9Ac}_2\alpha 2-3\text{Gal}$	-90 (-32)	10 (18)	
Gal $\beta$ 1-3GalNAc	-45 (25)	-30 (24)	
GalNAc $\beta$ 1-4Gal	30 (22)	10 (15)	
$^i\text{Neu5Ac}\alpha 2-3\text{Gal}$	-175 (26)	-20 (17)	
Gal $\beta$ 1-4Glc	30 (19)	-15 (18)	

Fig. 4. MD calculations of the  $\Phi$ ,  $\Psi$  angles of the glycosidic bonds within the oligosaccharide chain of  $G_{D1a}$  ( $^e\text{Neu5,9Ac}_2$ ) (fragment IV); (a) under explicit inclusion of water molecules in a box with periodic boundary conditions; (b) under explicit inclusion of water molecules only in a water layer and the use of a distance-dependent dielectric constant outside of the layer; (c) under explicit inclusion of DMSO molecules in a box with periodic boundary conditions; SD, standard deviation.



**Fig. 5.** Representation of the 15 structural units of  $G_{D1a}$  ( ${}^6\text{Neu5,9Ac}_2$ ) (a) and  $G_{D1a}$  (b) used for the calculation in the interaction analysis. Both gangliosides are subdivided into the corresponding parts, as illustrated in different colours. A, 9-*O*-acetyl group of the glycerol side chain of  ${}^6\text{Neu5,9Ac}_2$  (a) or 9-OH group of Neu5Ac (b); B, glycerol side chain of  ${}^6\text{sialic acid}$ ; C, *N*-acetyl side chain of  ${}^6\text{sialic acid}$ ; D, carboxyl group of  ${}^6\text{sialic acid}$ ; E,  ${}^6\text{sialic acid}$  without A, B, C, and D; F,  ${}^6\text{Gal}$ ; G, *N*-acetyl side chain of GalNAc; H, GalNAc without G; I,  ${}^1\text{Gal}$ ; J, glycerol side chain of  ${}^1\text{Neu5Ac}$ ; K, *N*-acetyl side chain of  ${}^1\text{Neu5Ac}$ ; L, carboxyl group of  ${}^1\text{Neu5Ac}$ ; M,  ${}^1\text{Neu5Ac}$  without J, K, and L; N, Glc; O, Cer.

a conformation that is significantly changed with regard to the non-*O*-acetylated ganglioside. Although a specific interaction of the 9-*O*-acetyl group with the *N*-acetylgalactosamine residue in  $G_{D1a}$  ( ${}^6\text{Neu5,9Ac}_2$ ) can be deduced, it does not yield a rigid conformation based on this contact and still allows a remarkable flexibility of the glycerol side chain of the outer sialic acid, as can also be deduced from the corresponding torsional angles.

Taking all these results together one possible conformation of  $G_{D1a}$  ( ${}^6\text{Neu5,9Ac}_2$ ) can be given, as depicted in Figure 7.

#### *Binding of $G_{D1a}$ ( ${}^6\text{Neu5,9Ac}_2$ ) to a 9-*O*-acetylated sialic acid-specific antibody preparation*

Although our results indicate that the conformations of  $G_{D1a}$  ( ${}^6\text{Neu5,9Ac}_2$ ) and  $G_{D1a}$  are very similar, the observable inter-

a)

	A	B	C	D	E	F	G	H	I	J	K	L	M	N	O
A	----	----	0.48	-0.06	-0.73	0.26	0.28	<b>-1.19</b>	0.63	-0.36	0.34	-0.09	-0.66	-0.07	-0.12
B	----	----	0.21	-0.62	----	-2.17	-0.43	0.79	-0.67	-1.76	-0.37	-0.18	-0.24	0.06	0.11
C	0.53	0.10	----	-0.25	----	0.55	0.35	-1.86	1.43	-0.60	-0.50	-1.22	<b>-3.76</b>	-0.14	-0.2
D	-0.02	0.03	-0.05	----	----	2.72	-0.03	0.01	-0.02	-0.02	-0.01	-0.01	-0.02	0.00	0.00
E	-0.57	----	----	----	----	----	-0.80	1.77	-1.71	-0.11	-0.68	-1.15	1.19	0.15	0.27
F	0.42	-0.74	0.76	3.91	----	----	0.73	----	1.69	-0.23	0.48	-1.15	-1.27	-0.24	-0.28
G	0.30	-0.32	0.41	-0.01	-0.51	1.48	----	----	0.63	-0.19	0.41	-1.11	-1.59	-0.72	-0.35
H	<b>-0.96</b>	1.31	-1.78	0.04	2.02	----	----	----	----	<b>-2.44</b>	-1.29	-0.81	1.41	0.58	0.59
I	0.65	-0.58	1.52	-0.01	-1.61	1.96	3.22	----	----	-1.59	1.03	2.65	----	----	-0.93
J	0.31	-0.68	-0.23	0.00	0.07	-0.03	-0.04	<b>0.10</b>	-0.20	----	0.36	-0.91	----	0.02	0.02
K	0.37	-0.23	0.67	0.00	-0.59	0.50	0.43	-1.23	1.19	0.39	----	-0.28	----	-0.10	-0.23
L	-0.06	0.20	-0.18	0.03	0.20	-0.32	0.06	0.24	3.96	-0.07	-0.05	----	----	-0.03	-0.01
M	-0.61	0.28	<b>-2.43</b>	0.00	1.62	-1.06	-0.74	2.47	----	----	----	----	----	0.16	0.36
N	-0.06	0.06	-0.13	0.00	0.15	-0.23	-0.56	0.68	----	0.04	-0.09	0.00	0.26	----	----
O	-0.12	0.11	-0.20	0.00	0.27	-0.27	-0.34	0.59	-0.78	0.02	-0.22	0.00	0.37	----	----

b)

	A	B	C	D	E	F	G	H	I	J	K	L	M	N	O
A	----	----	0.55	-0.11	-0.96	-0.69	0.44	<b>-4.22</b>	0.83	-1.02	0.34	-1.02	-1.27	-0.13	-0.13
B	----	----	-1.74	-0.75	----	-1.63	-0.40	0.54	0.70	-0.65	-0.62	-1.07	-0.29	0.07	0.10
C	0.60	-1.87	----	-0.27	----	0.85	0.34	-1.47	1.18	0.01	0.30	-0.24	<b>-2.63</b>	-0.17	-0.18
D	-0.02	0.04	-0.06	----	----	3.34	-0.05	0.01	-0.02	-0.01	-0.02	-0.04	0.01	0.00	0.00
E	-0.65	----	----	----	----	----	-0.97	1.70	-1.49	-0.12	-0.62	-1.20	1.14	0.18	0.25
F	0.65	-0.25	1.00	3.89	----	----	-0.65	----	0.92	-0.05	0.42	-1.50	-1.26	-0.19	-0.23
G	0.57	-0.27	0.38	-0.01	-0.65	1.26	----	----	0.43	-0.02	0.33	-1.28	-1.16	-0.34	-0.24
H	<b>-2.35</b>	0.87	-1.44	0.04	1.86	----	----	----	----	<b>-3.54</b>	-1.29	-0.84	1.35	0.56	0.52
I	0.96	-0.58	1.22	-0.01	-1.41	1.24	1.48	----	----	-1.26	0.89	2.76	----	----	-0.77
J	0.39	-0.06	0.06	0.00	-0.06	0.08	0.08	<b>-1.23</b>	0.20	----	-0.93	-0.78	----	-0.05	-0.01
K	0.41	-0.33	0.55	-0.01	-0.56	0.45	0.35	-1.23	1.06	-0.94	----	-0.28	----	-0.20	-0.21
L	-0.39	-0.27	0.10	0.01	-0.25	-0.39	-0.21	0.30	4.03	0.00	-0.06	----	----	-0.04	-0.01
M	-0.93	0.90	<b>-1.89</b>	0.03	1.46	-0.98	-0.47	2.47	----	----	----	----	----	0.24	0.31
N	-0.12	0.08	-0.17	0.00	0.18	-0.17	-0.26	0.65	----	-0.02	-0.19	-0.02	0.35	----	----
O	-0.13	0.11	-0.18	0.00	0.25	-0.22	-0.23	0.52	-0.69	0.00	-0.21	-0.01	0.32	----	----

**Fig. 6.** Values of the sum of van der Waals energy and Coulomb energy (part above diagonal separation) and of the Coulomb energy alone given in kcal/mol (part below diagonal separation) of the structural elements A–O (Figure 5) of G<sub>D1a</sub> (<sup>6</sup>Neu5,9Ac<sub>2</sub>) (a and b) and for G<sub>D1a</sub> (c and d) derived from corresponding MD calculations after simulation times of 500 ps (a and c) and 1000 ps (b and d). A, 9-*O*-acetyl group of the glycerol side chain of <sup>6</sup>Neu5,9Ac<sub>2</sub> (a and b) or 9-OH group of the glycerol chain of <sup>6</sup>Neu5Ac (c and d); B, glycerol side chain of <sup>6</sup>sialic acid; C, *N*-acetyl side chain of <sup>6</sup>sialic acid; D, carboxyl group of <sup>6</sup>sialic acid; E, <sup>6</sup>sialic acid without A, B, C, and D; F, <sup>1</sup>Gal; G, *N*-acetyl side chain of GalNAc; H, GalNAc without G; I, <sup>6</sup>Gal; J, glycerol side chain of <sup>1</sup>Neu5Ac; K, *N*-acetyl side chain of <sup>1</sup>Neu5Ac; L, carboxyl group of <sup>1</sup>Neu5Ac; M, <sup>1</sup>Neu5Ac without J, K, and L; N, Glc; O, Cer.

action between the 9-*O*-acetyl group and the pyranose ring of the *N*-acetylgalactosamine residue in the simulation may also indicate the occurrence of a distinct position of these chain constituents within one possible conformer (Figure 7). To explain preferential binding of 9-*O*-acetylated sialic acid derivatives to receptor proteins on a molecular level, this functional

group must be accessible to the binding protein like the polyclonal IgG fraction from human serum used in this study in order to serve as a docking place for a corresponding receptor. To provide evidence for such an interaction, one-dimensional <sup>1</sup>H-NMR-spectra of G<sub>D1a</sub> (<sup>6</sup>Neu5,9Ac<sub>2</sub>) in D<sub>2</sub>O/DPC in the absence and presence of the antibody fraction were recorded.

c)

	A	B	C	D	E	F	G	H	I	J	K	L	M	N	O
A	----	----	0.25	-0.03	-0.45	-0.13	0.07	<b>-0.57</b>	0.18	-0.43	0.05	-0.12	-0.25	-0.03	-0.03
B	----	----	0.42	-0.70	----	-1.55	-0.15	-0.40	0.00	-1.21	-0.17	-1.02	-0.44	-0.01	0.01
C	0.31	0.35	----	-0.26	----	0.55	0.36	-1.94	1.10	-0.75	-0.49	-1.30	<b>-3.72</b>	-0.20	-0.21
D	-0.01	-0.05	-0.04	----	----	2.68	-0.04	0.01	-0.01	-0.02	0.00	-0.01	-0.03	0.00	0.00
E	-0.30	----	----	----	----	----	-1.00	2.30	-1.88	0.10	-0.84	-2.15	1.45	0.27	0.32
F	0.00	-0.16	0.76	3.84	----	----	0.42	----	1.51	-0.37	0.48	-1.12	-1.33	-0.33	-0.29
G	0.08	-0.05	0.43	0.00	-0.50	1.17	----	----	0.65	-0.28	0.43	-1.15	-1.66	-0.83	-0.34
H	<b>-0.45</b>	-0.05	-1.86	0.05	2.56	----	----	----	----	<b>-2.82</b>	-1.33	-0.78	1.40	0.62	0.53
I	0.19	0.07	1.20	0.00	-1.75	1.79	3.16	----	----	-1.74	0.81	2.52	----	----	-0.99
J	-0.05	-0.47	-0.36	0.00	0.29	-0.15	-0.12	<b>-0.15</b>	-0.22	----	0.09	-0.99	----	0.08	0.03
K	0.06	-0.05	0.63	0.00	-0.74	0.50	0.45	-1.27	0.98	0.14	----	-0.27	----	-0.20	-0.26
L	-0.08	-0.44	-0.16	0.04	-0.48	-0.32	0.04	0.29	3.85	-0.10	-0.04	----	----	-0.02	-0.01
M	-0.21	-0.01	<b>-2.31</b>	-0.01	2.04	-1.10	-0.83	2.48	----	----	----	----	----	0.33	0.43
N	-0.03	-0.01	-0.20	0.00	0.28	-0.31	-0.68	0.73	----	0.10	-0.19	0.01	0.43	----	----
O	-0.03	0.01	-0.21	0.00	0.32	-0.28	-0.33	0.54	-0.91	0.04	-0.26	-0.01	0.44	----	----

d)

	A	B	C	D	E	F	G	H	I	J	K	L	M	N	O
A	----	----	0.13	-0.01	-0.17	0.07	0.09	<b>-0.38</b>	0.19	0.04	0.09	-0.04	-0.17	-0.01	-0.04
B	----	----	0.47	-0.63	----	-1.89	-0.20	0.17	-0.23	-1.12	-0.10	-0.52	-0.54	0.01	0.04
C	0.15	0.40	----	-0.24	----	0.62	0.34	-1.89	1.39	-0.74	-0.27	-1.36	<b>-3.80</b>	-0.15	-0.23
D	0.01	0.03	-0.04	----	----	2.65	-0.04	0.01	-0.01	-0.02	-0.01	-0.01	-0.04	0.00	0.00
E	-0.09	----	----	----	----	----	-0.90	1.88	-1.82	0.06	-0.77	-1.39	1.49	0.14	0.32
F	0.13	-0.50	0.84	3.83	----	----	0.76	----	1.88	-0.20	0.52	-1.14	-1.35	-0.32	-0.47
G	0.09	-0.10	0.41	-0.01	-0.51	1.57	----	----	0.71	-0.08	0.42	-1.20	-1.58	-3.71	-0.67
H	<b>-0.35</b>	0.57	-1.81	0.04	2.13	----	----	----	----	<b>-2.52</b>	-1.33	-0.80	1.38	0.30	0.77
I	0.19	-0.16	1.49	0.00	-1.71	2.17	3.27	----	----	-1.66	0.85	2.56	----	----	-1.09
J	0.08	-0.27	-0.39	-0.01	0.22	-0.02	0.06	<b>0.17</b>	-0.06	----	-1.50	-1.00	----	-0.01	-0.02
K	0.10	0.01	0.77	0.00	-0.69	0.54	0.45	-1.27	1.03	-1.41	----	-0.28	----	-0.11	-0.22
L	-0.03	0.03	-0.14	0.04	0.15	-0.28	0.01	0.27	3.89	-0.12	-0.05	----	----	-0.07	0.00
M	-0.16	-0.11	<b>-2.43</b>	-0.02	1.98	-1.14	-0.74	2.46	----	----	----	----	----	0.15	0.40
N	-0.01	0.02	-0.14	0.00	0.16	-0.24	-1.67	0.71	----	0.03	-0.10	0.00	0.29	----	----
O	-0.04	0.04	-0.23	0.00	0.33	-0.43	-0.59	0.84	-0.97	-0.01	-0.22	0.00	0.41	----	----

Fig. 6. Continued

As shown in Figure 8, a and b, the signal of the methyl signal from the 9-*O*-acetyl group almost disappears after addition of the antibody fraction (Figure 8b) when compared to the starting conditions without added receptor (Figure 8a). When this antibody fraction is incubated with the monosaccharide Neu5,9Ac<sub>2</sub>, a considerable line broadening is seen. In the case of non-*O*-acetylated Neu5Ac and Neu5Gc monosaccharides, no significant line broadening could be detected. Hence, it can be concluded that the methyl protons of the 9-*O*-acetyl group of Neu5,9Ac<sub>2</sub> specifically interact with amino acids in the binding site of the protein. The fact that the intramolecular

interactions of G<sub>D1a</sub> (°Neu5,9Ac<sub>2</sub>) are not strong enough to preferentially establish one conformation with the 9-*O*-acetyl substituent buried within the molecule guarantees that this group is accessible for an intermolecular recognition processes, providing a measurable contact region for a 9-*O*-acetyl-recognising domain of a receptor.

#### Conclusion

The computer-assisted generation of oligosaccharide fragments as parts of a more complicated structure, newly introduced in



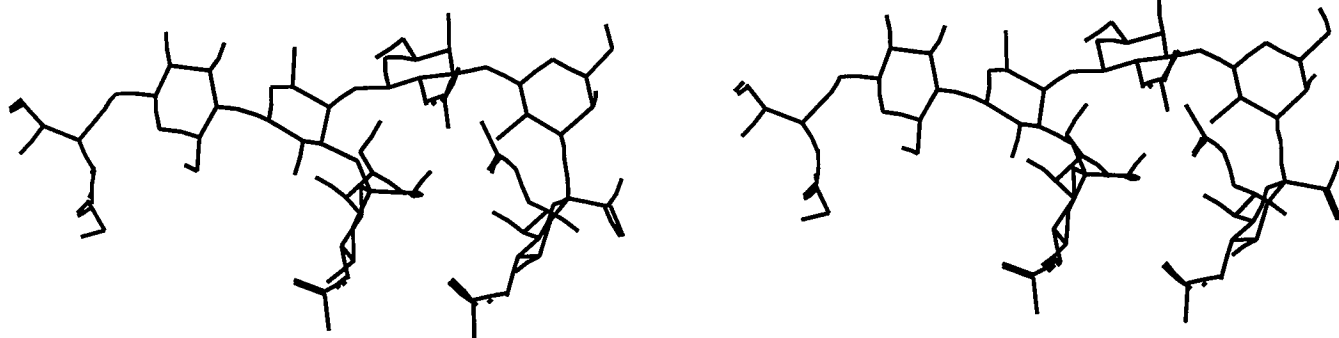


**Fig. 7.** Stereo plot of  $G_{D1a}$  ( ${}^e\text{Neu5,9Ac}_2$ ), representing the conformation as deduced from MD calculations of fragment IV after 1000 ps and the corresponding data from the interaction analysis.

this investigation, followed by MD calculations of these partial structures proved to be very helpful in studying the influence of individual residues on the total saccharide conformation and dynamic behaviour, as did the interaction analysis that was also developed for the present study, and allows recognition of interactions that cannot be detected as direct NOE contacts. This approach enabled delineation of conformations for such a complex branched molecule like  $G_{D1a}$  ( ${}^e\text{Neu5,9Ac}_2$ ).

On this structural basis, inherent flexibility and at least partial accessibility of the 9-*O*-acetyl group of  $G_{D1a}$  ( ${}^e\text{Neu5,9Ac}_2$ )

could be deduced for the oligosaccharide chain. The experimental proof for the assumed accessibility of this group for a receptor was accomplished by NMR measurements with the ganglioside and a 9-*O*-acetyl-binding IgG fraction from human serum revealing the participation of the methyl protons of the 9-*O*-acetyl group in this recognition process. With these tools in hands, we will be able to further investigate carbohydrate-protein interactions in solution on a molecular level and set a basis for an improved understanding of many fundamental biological processes, which also may have relevance for clinical

### $e\text{N9-O-Ac}$

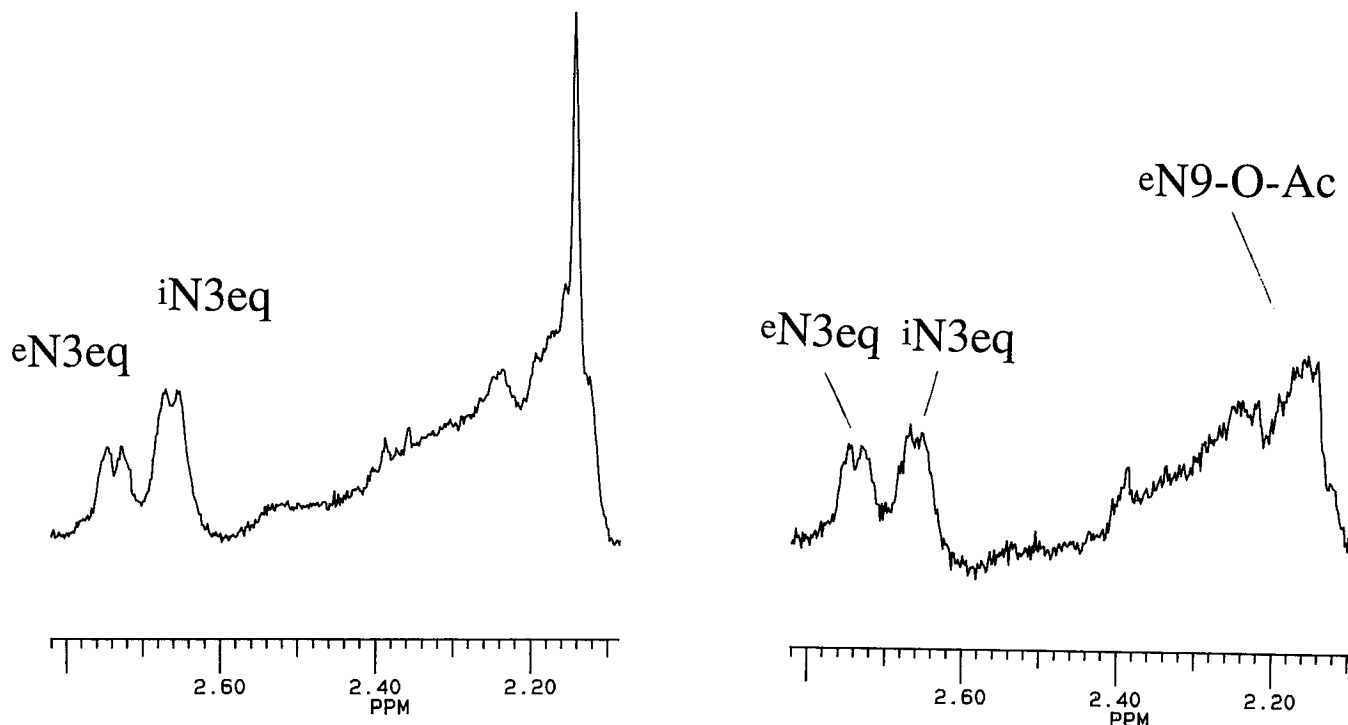


**Fig. 8.** NMR-signal of the 9-*O*-acetyl group of  $G_{D1a}$  ( ${}^e\text{Neu5,9Ac}_2$ ) (1 mg). (a) In the free state; (b) after addition of 4 mg of the affinity-purified polyclonal IgG fraction with preferential affinity to 9-*O*-acetylated sialic acids; for comparison, the signals of the  $\text{H}_{3_{eq}}$  of both sialic acids  ${}^e\text{Neu5,9Ac}_2$  and  ${}^i\text{Neu5Ac}$  are also given.

applications (Gabius *et al.*, 1995; Gabius, 1996; Gabius and Gabius, 1996).

## Material and methods

Deuterated solvents ( $D_2O$  and  $DMSO-d_6$ ; both 99.96 atom % D) and the detergent dodecylphosphocholine- $d_{38}$  (DPC- $d_{38}$ ) were purchased from Merck, Sharp and Dohme (Montreal, Canada). Neu5Ac and Neu5Gc were isolated from bovine submandibular gland mucin (Reuter *et al.*, 1983). Neu5,9Ac<sub>2</sub> was obtained from Neu5Ac by treatment with trimethyl orthoacetate according to a published procedure (Ogura *et al.*, 1987).  $G_{D1a}$  and  $G_{D1a}$  (<sup>c</sup>Neu5,9Ac<sub>2</sub>) were isolated from red blood cells of Wistar and CAP rats, following a well-established procedure (Leeden and Yu, 1982; Gowda *et al.* 1984).

### Preparation of polyclonal antibody fraction

Human serum from normal donors served as source to purify the polyclonal antibody (IgG) fraction with preferential affinity to *O*-acetylated sialic acids (Ahmed and Gabius, 1989; Zeng and Gabius, 1992; Zeng *et al.*, 1992). In brief, after removal of any serum components with affinity to the Sepharose 4B matrix and of any galactose-binding proteins by affinity chromatography over lactose-bearing Sepharose 4B the resulting serum fraction was passed over the affinity matrix constituted by immobilisation of bovine submandibular gland mucin to divinyl sulfone-activated Sepharose 4B (Ahmed and Gabius, 1989) and eluted with 0.1 M  $NH_4OH$  (pH 11) followed by immediate neutralisation. After affinity chromatography over protein A-Sepharose 4B, an IgG fraction was obtained, which nearly exclusively comprises IgG<sub>2</sub>. The eluted protein was dialysed against phosphate-buffered saline and finally against water and lyophilised. The protein content was determined by the dye-binding assay adapted for microtiter plates (Redinbaugh and Campbell, 1985) using bovine serum albumin as reference.

### NMR measurements

For the preparation of mixed micelles (Eaton and Hakomori, 1988; Siebert *et al.*, 1992), the purified gangliosides  $G_{D1a}$  and  $G_{D1a}$  (<sup>c</sup>Neu5,9Ac<sub>2</sub>) (2 mg, each) and DPC- $d_{38}$  were mixed in deuterated potassium phosphate buffer at pD 6 in a molar ratio of 1:40. The solvent was exchanged twice with  $D_2O$ , with intermediate lyophilization, and the sample was dried in high vacuum and finally dissolved in 0.4 ml of  $D_2O$  for NMR measurements. In addition, mixed micelles of  $G_{D1a}$  and  $G_{D1a}$  (<sup>c</sup>Neu5,9Ac<sub>2</sub>), and DPC- $d_{38}$  in  $D_2O$  (corresponding to 2 mg ganglioside) were incubated with the affinity-purified antibody fraction (4 mg of protein) before analysis. In another series of NMR experiments the gangliosides  $G_{D1a}$  and  $G_{D1a}$  (<sup>c</sup>Neu5,9Ac<sub>2</sub>) (2 mg each), which had been dried in high vacuum, were dissolved in 0.4 ml of  $DMSO-d_6$  for performing NMR studies (Siebert, 1990). All NMR spectra were obtained at a frequency of 500 MHz on a Bruker AM-500 spectrometer equipped with an Aspect 3000 computer and process controller.

### Molecular dynamics calculations

The oligosaccharide parts of  $G_{D1a}$  and  $G_{D1a}$  (<sup>c</sup>Neu5,9Ac<sub>2</sub>) were generated by successively linking the appropriate monosaccharides to the chain starting from the non-reducing end with the aid of the SUGAR program of the CARBYD interface (von der Lieth *et al.*, 1989). The coordinates for the sugar ring atoms were taken from the Cambridge Crystallographic Data Bank. Substitution of the exocyclic groups was accomplished with the aid of the MOLBUILD program (Liliefors, 1983). The MM calculations were run on an IBM 3090 computer with the use of the standard MM2(87) force field (Burkert and Allinger, 1982; Allinger *et al.*, 1988) and a dielectric constant  $\epsilon = 4$ . The conformations which represent energy minima were used as geometrical starting points for MD calculations. The Consistence Valence Force Field (CVFF) (Hagler *et al.*, 1974, 1979a,b) implemented in the DISCOVER 2.9 program (Biosym Technologies, San Diego, USA) was employed for the MD calculations. Input files for DISCOVER were prepared following the automatic charge and parameter assignment procedure of INSIGHT-III. For the interaction analysis the 9-*O*-acetylated and non-*O*-acetylated  $G_{D1a}$ -molecules were divided into 15 structurally meaningful features, as shown in detail in Figure 5. Over the whole simulation time of 1000 ps, 20 structures were drawn from a MD simulation by storing and minimising a conformation after every 50 ps. The interaction energies (van der Waals and Coulomb interactions) were calculated between all defined parts of the molecule. The interaction analysis was accomplished using the RESIDUE-RESIDUE INTERACTION option of the PRINT command of DISCOVER.

MD-simulations in vacuum were carried out at simulation temperatures of

300 K or 400 K and dielectric constants  $\epsilon$  of 4 or 80; a dielectric constant of 80 is equivalent to that of water. No additional forces or non-bonded cut-offs were applied during the simulation. The molecules were equilibrated for 10 ps and remained at a thermal equilibrium at this temperature for the rest of the simulation. The generation of the various trajectories was done with the ANALYSIS option of INSIGHT. The trajectories were plotted and examined with the program DISANA (our own software). All MD calculations were run on a CONVEX C3440 computer.

In addition two different simulation protocols with explicit inclusion of water molecules were performed for the complete  $G_{D1a}$  (<sup>c</sup>Neu5,9Ac<sub>2</sub>) oligosaccharide chain, namely periodic boundary conditions as well as water layers and a distance-dependent dielectric constant of  $\epsilon = 1/r$  (Guenot and Kollman, 1992, 1993). Both solvation models were generated with the SOAK option of INSIGHT II. The details for the simulation using periodic boundary conditions were as follows: simple point charges for the water molecule models, 631 water molecules, unit cell dimensions of  $x = 35 \text{ \AA}$ ,  $y = 25 \text{ \AA}$ , and  $z = 25 \text{ \AA}$ , angles  $\alpha = \beta = \gamma = 90^\circ$ ; equilibrium time 50 ps at 300 K and state of thermal equilibrium for the rest of the simulation. A 5  $\text{\AA}$  thick layer of water molecules around  $G_{D1a}$  (<sup>c</sup>Neu5,9Ac<sub>2</sub>) was generated and applied in conjunction with a distance-dependent dielectric constant. A time integration step of 0.1 fs and a cut-off distance of non-bonded interactions of 12  $\text{\AA}$  were chosen. Additionally, MD-simulations in the solvent DMSO were carried out using the model solvent of Mierke and Kessler (1992) under the following conditions: periodic boundary, simple point charges for the DMSO molecule models, 288 DMSO molecules, unit cell dimensions of  $x = 35 \text{ \AA}$ ,  $y = 35 \text{ \AA}$ , and  $z = 35 \text{ \AA}$ , angles  $\alpha = \beta = \gamma = 90^\circ$ ; equilibrium time 50 ps at 300 K and state of thermal equilibrium for the rest of the simulation. All simulations in the presence of solvent molecules were performed on an IBM-SP2 parallel machine using the parallel version of DISCOVER and four processors.

Dihedral angles  $\Phi$  and  $\Psi$  are defined as follows.  $\Phi$ : C1-C2-O-C3,  $\Psi$ : C2-O-C3-H3 for Neu5Ac $\alpha$ 2-3Gal;  $\Phi$ : H1-C1-O-CX,  $\Psi$ : C1-O-CX-HX for the other glycosidic linkages.  $\Phi$  correspond to  $\Phi_{H}$ ;  $\Psi$  correspond to  $\Psi_{H}$  according to the IUPAC conventions. The angles describing the 9-*O*-acetylated glycerol side chain of the external sialic acid are  $\omega'_6$ , H6-C6-C7-H7;  $\omega'_7$ , H7-C7-C8-H8;  $\omega'_8$ , H8-C8-C9-O9;  $\omega'_9$ , C8-C9-O9-C10; and  $\omega'_{10}$ , C9-O9-C10-C11, with C10 being the carbonyl C atom of the 9-*O*-acetyl group and C11 as methyl C atom of this substituent. The angles of the non-*O*-acetylated glycerol side chain,  $\omega_6$ ,  $\omega_7$ ,  $\omega_8$ , are defined analogously. All torsion angles listed in the Figures 2 and 4 are averaged values from the trajectories.

## Acknowledgements

This investigation was supported by the Human Capital and Mobility Program of the European Community, the Dr.-M.-Scheel-Stiftung für Krebsforschung and by the Netherlands Foundation for Chemical Research (SON). We sincerely thank Prof. Dr. Janusz Dabrowski from the Max-Planck-Institut für Medizinische Forschung in Heidelberg for highly esteemed help and many fruitful discussions; Prof. Dr. Dr. Heinz Staab, head of the Department of Organic chemistry at the Max-Planck-Institut für Medizinische Forschung, for valuable access to the 500 MHz-NMR spectrometer; and Dr. Dale F. Mierke and Prof. Dr. Horst Kessler from the Technische Universität München, Organisch-Chemisches Institut, for making available to us the software for MD calculations including DMSO as solvent.

## Abbreviations

DPC, dodecylphosphocholine;  $G_{D1a}$  (<sup>c</sup>Neu5,9Ac<sub>2</sub>),  $G_{D1a}$  with *N*-acetyl-9-*O*-acetylneuraminic acid bound to the external galactose residue; <sup>i</sup>Neu5Ac in  $G_{D1a}$  or  $G_{D1a}$  (<sup>c</sup>Neu5,9Ac<sub>2</sub>), *N*-acetylneuraminic acid bound to the internal galactose residue; Neu5Ac, *N*-acetylneuraminic acid; Neu5,9Ac<sub>2</sub>, *N*-acetyl-9-*O*-acetylneuraminic acid; Neu5Gc, *N*-glycolylneuraminic acid.

## References

- Acquotti, D., Cantu, L., Ragg, E. and Sonnino, S. (1994) Geometrical and conformational properties of ganglioside GalNAc- $G_{D1a}$ , IV<sup>4</sup>GalNAcIV<sup>3</sup>NeuAcII<sup>3</sup>Neu5AcGgOse<sub>4</sub>Cer. *Eur. J. Biochem.*, **225**, 271-288.
- Ahmed, H. and Gabius, H.-J. (1989) Purification and properties of a Ca<sup>2+</sup>-independent sialic acid-binding lectin from human placenta with preferential affinity to *O*-acetylated sialic acids. *J. Biol. Chem.*, **264**, 18673-18678.
- Allinger, N.L., Kok, R.A. and Imam, M.R. (1988) Hydrogen bonding in MM2. *J. Comput. Chem.*, **9**, 591-595.
- Asensio, J., Martin-Pastor, M. and Jimenez-Babero, J. (1995) The use of CVFF and CVFF91 force fields in conformational analysis of carbohydrate mol-

- ecules. Comparison with AMBER molecular mechanics and dynamics calculations for methyl  $\alpha$ -lactoside. *Int. J. Biol. Macromol.*, **17**, 137–148.
- Balaji,P.V., Qasba,P.K. and Rao,V.S.R. (1993) Molecular dynamics simulations of asialo-glycoprotein. *Biochemistry*, **32**, 12599–12611.
- Balaji,P.V., Qasba,P.K. and Rao,V.S.R. (1994) Molecular dynamics simulations of high-mannose oligosaccharides. *Glycobiology*, **4**, 497–515.
- Burkert,U. and Allinger,N.L. (1982) *Molecular Mechanics*, American Chemical Society, Washington, DC.
- Cheresh,D.A., Reisfeld,R.A. and Varki,A.P. (1984a) *O*-Acetylation of disialoganglioside G<sub>D3</sub> by human melanoma cells creates a unique antigenic epitope. *Science*, **225**, 844–846.
- Cheresh,D.A., Varki,A.P., Varki,N.M., Stallcup,W.B., Levine,J. and Reisfeld,R.A. (1984b) A monoclonal antibody recognizes an *O*-acetylated sialic acid in a human melanoma-associated ganglioside. *J. Biol. Chem.*, **259**, 7453–7459.
- Eaton,H.L. and Hakomori,S. (1988) Conformation of micelle-bound gangliosides by 2D proton NMR spectroscopy. *Third Chemical Congress of North America*, Abstract CARB 91, Toronto.
- Gabius,H.-J. (1996) Concepts of tumor lectinology. *Cancer Invest.*, in press
- Gabius,H.-J. and Gabius,S. (1996) *Glycosciences: Status and Perspectives*. Chapman & Hall, Weinheim.
- Gabius,H.-J., Kayser,K. and Gabius,S. (1995) Protein-Zucker-Erkennung. Grundlagen und medizinische Anwendung am Beispiel der Tumorlektinologie. *Naturwissenschaften*, **82**, 533–543.
- Gowda,D.C., Reuter,G., Shukla,A.K. and Schauer,R. (1984) Identification of a disialoganglioside (G<sub>D1a</sub>) containing terminal *N*-acetyl-9-*O*-acetylneuraminic acid in rat erythrocytes. *Hoppe-Seyler's Z. Physiol. Chem.*, **365**, 1247–1253.
- Guenot,J. and Kollman,P.A. (1992) Molecular dynamics studies of DNA-binding protein: an evaluation of implicit and explicit solvent models for the molecular dynamics simulation of the *Escherichia coli* trp repressor. *Protein Sci.*, **1**, 1185–1205.
- Guenot,J. and Kollman,P.A. (1993) Conformational and energetic effects of truncating nonbonded interactions in an aqueous protein dynamics simulation. *J. Comput. Chem.*, **14**, 278–284.
- Hagler,A.T., Huler,E. and Lifson,S. (1974) Energy functions for peptides and proteins. Deviation of a consistent force field including the hydrogen bond for amide crystals. *J. Am. Chem. Soc.*, **96**, 5316–5327.
- Hagler,A.T., Lifson,S. and Dauber,P. (1979a) Consistent force field studies of intermolecular forces in hydrogen-bonded crystals. 2. A benchmark for the objective comparison of alternative force fields. *J. Am. Chem. Soc.*, **101**, 5122–5130.
- Hagler,A.T., Dauber,P., and Lifson,S. (1979b) Consistent force field studies of intermolecular forces in hydrogen-bonded crystals. 3. The C=O···H-O hydrogen bond and the analysis of the energetics and packing of carboxylic acids. *J. Am. Chem. Soc.*, **101**, 5131–5141.
- Hakomori,S. (1990) Bifunctional role of glycosphingolipids. *J. Biol. Chem.*, **265**, 18713–18716.
- Hakomori,S. (1991) New directions in cancer therapy based on aberrant expression of glycosphingolipids: anti-adhesion and ortho-signalling therapy. *Cancer Cells*, **3**, 461–470.
- Herrler,G., Rott,R., Klenk,H.D., Müller,H.P., Shukla,A.K. and Schauer,R. (1985) The receptor-destroying enzyme of influenza C virus is neuraminidase-*O*-acetyltransferase. *EMBO J.*, **4**, 1503–1506.
- Homans,S.W. (1990) A molecular mechanical force field for the conformational analysis of oligosaccharides: comparison of theoretical and crystal structures of Man $\alpha$ 1–3 Man $\beta$ 1–4 GlcNAc. *Biochemistry*, **92**, 9110–9118.
- Kelm,S., Schauer,R., Manuguerra,J.C., Gross,H.-J. and Crocker,P. (1994) Modification of cell surface sialic acids modulate cell adhesion mediated by sialoadhesin and CD22. *Glycoconjugate J.*, **11**, 576–585.
- Klein,A., Krishna,M., Varki,N.M. and Varki,A. (1994) 9-*O*-Acetylated sialic acids have widespread but selective expression: analysis using a chimeric dual-function probe derived from influenza C hemagglutinin-esterase. *Proc. Natl. Acad. Sci. USA*, **91**, 7782–7786.
- Kopitz,J. (1996) Glycolipids: structure and functions. In Gabius,H.-J. and Gabius,S. (eds.), *Glycosciences: Status and Perspectives*. Chapman & Hall, Weinheim, in press.
- Kozár,T. (1995) Force fields. *First Electronic Glycoscience Conference*.
- Ledeer,R.W. and Yu,R.K. (1982) Gangliosides: structure, isolation and analysis. *Methods Enzymol.*, **83**, 139–191.
- Liliefors,M. (1983) MOLBUILD—an interactive computer graphics interface to molecular mechanics. *J. Mol. Graphics*, **1**, 111–117.
- Manzi,A.E., Sjoberg,E.R., Diaz,S. and Varki,A. (1990) Biosynthesis and turnover of *O*-acetyl and *N*-acetyl groups in the gangliosides of human melanoma cells. *J. Biol. Chem.*, **265**, 13091–13103.
- Marti,J., Guàrdia,E., and Padró,J.A. (1994) Dielectric properties and infrared spectra of liquid water: influence of the dynamic cross correlations. *J. Chem. Phys.*, **101**, 10883–10891.
- Mierke,D. and Kessler,H. (1992) Combined use of homo- and heteronuclear coupling constants as restraints in molecular dynamics simulations. *Biopolymers*, **32**, 1277–1282.
- Ogura,H., Furuhashi,K., Sato,S., Anazawa,K., Itoh,M. and Shitory,Y. (1987) Synthesis of 9-*O*-acetyl- and 4-*O*-acetyl-sialic acids. *Carbohydr. Res.*, **167**, 77–86.
- Poppe,L., van Halbeek,H., Acquotti,D., Sonnio,S. and Tettamanti, G. (1994) Carbohydrate dynamics at a micellar surface: G<sub>D1a</sub> headgroup transformations revealed by NMR spectroscopy. *Biophys. J.*, **66**, 1642–1652.
- Ravindranath,M.H., Paulson,J.C. and Irie,R.F. (1988) Human melanoma antigen *O*-acetylated ganglioside G<sub>D3</sub> is recognized by *Cancer antennarius* lectin. *J. Biol. Chem.*, **263**, 2079–2086.
- Ravindranath,M.H., Morton,D.L. and Irie,R.F. (1989) An epitope common to gangliosides *O*-acetyl-G<sub>D3</sub> and G<sub>D3</sub> recognized by antibodies in melanoma patients after active specific immunotherapy. *Cancer Res.*, **49**, 3891–3897.
- Redinbaugh,M.E. and Campbell,W.H. (1985) Adaptation of the dye-binding protein assay to microtiter plates. *Anal. Biochem.*, **147**, 144–147.
- Reuter,G. and Schauer,R. (1987) Isolation and analysis of gangliosides with *O*-acetylated sialic acids. In Rahmann,H. (ed.), *Gangliosides and Modulation of Neuronal Functions*, NATO ASI Series H. Springer Verlag, Heidelberg, pp. 155–167.
- Reuter,G., Pfeil,R., Stoll,S., Schauer,R., Kamerling,J.P., Versluis,C. and Vliegthart,J.F.G. (1983) Identification of new sialic acids derived from glycoprotein of bovine submandibular gland. *Eur. J. Biochem.*, **134**, 139–143.
- Ritter,G., Livingston,P.O., Boosfeld,E., Wiegandt,H., Yu,R.K., Oettgen,H.F. and Old,L.J. (1989) Development of melanoma vaccines: gangliosides as immunogens. In Oettgen,H.F. (ed.), *Gangliosides and Cancer*. VCH, Weinheim, pp. 301–313.
- Ritter,G., Boosfeld,E., Markstein,E., Yu,R.K., Ren,S., Stallcup,W.B., Oettgen,H.F., Old,L.J. and Livingston,P.O. (1990) Biochemical and serological characteristics of natural 9-*O*-acetyl G<sub>D3</sub> from human melanoma and bovine buttermilk and chemically *O*-acetylated G<sub>D3</sub>. *Cancer Res.*, **50**, 1403–1410.
- Sabesan,S., Duus,J., Fukunaga,T., Bock,K. and Ludvigsen,S. (1991a) NMR and conformational analysis of ganglioside G<sub>D1a</sub>. *J. Am. Chem. Soc.*, **113**, 3236–3246.
- Sabesan,S., Bock,K. and Paulson,J.C. (1991b) Conformational analysis of sialyloligosaccharides. *Carbohydr. Res.*, **218**, 27–54.
- Scarsdale,J.N., Prestegard,J.H. and Yu,R.K. (1990) NMR and computational studies of interactions between remote residues in gangliosides. *Biochemistry*, **29**, 9843–9855.
- Schauer,R. (1979) Biosynthesis of sialic acids. *Methods Enzymol.*, **50**, 374–386.
- Schauer,R. (1982) Chemistry, metabolism and biological functions of sialic acids. *Adv. Carbohydr. Chem. Biochem.*, **40**, 131–234.
- Schauer,R., Kelm,S., Reuter,G., Roggentin,P. and Shaw,L. (1995) Biochemistry and role of sialic acids. In Rosenberg,A. (ed.), *Biology of the Sialic Acids*. Plenum Press, New York, pp. 7–67.
- Schultze,B., Zimmer,G. and Herrler,G. (1993) Viral lectins for the detection of 9-*O*-acetylated sialic acid on glycoproteins and glycolipids. In Gabius,H.-J. and Gabius,S. (eds.), *Lectins and Glycobiology*. Springer Verlag, Heidelberg, pp. 175–181.
- Siebert,H.C. (1990) *Konformationsanalyse verschiedener Ganglioside mit Hilfe von <sup>1</sup>H-Kernresonanzmethoden und Computerberechnungen*. Ph.D. Thesis, University of Heidelberg.
- Siebert,H.C., Reuter,G., Schauer,R., von der Lieth,C.W. and Dabrowski,J. (1992) Solution conformation of G<sub>M3</sub> gangliosides containing different sialic acid residues as revealed by NOE-based distance-mapping, and molecular mechanics and molecular dynamics calculations. *Biochemistry*, **31**, 6962–6971.
- Siebert,H.-C., Kaptein,R. and Vliegthart,J.F.G. (1993) Study of oligosaccharide-lectin interaction by various nuclear magnetic resonance (NMR) techniques and computational methods. In Gabius,H.-J. and Gabius,S. (eds.), *Lectins and Glycobiology*, Springer Verlag, Heidelberg, pp. 105–116.
- Siebert,H.-C., Gilleron,M., Kaltner,H., von der Lieth,C.-W., Kozár,T., Bovic,N.V., Korchagina,E.Y., Vliegthart,J.F.G. and Gabius H.-J. (1996a) NMR-based, molecular dynamics- and random walk molecular mechanics-supported study of conformational aspects of a carbohydrate ligand (Gal $\beta$ 1,2Gal $\beta$ 1-R) for an animal galectin in the free and in the bound state. *Biochem. Biophys. Res. Commun.*, **219**, 205–212.
- Siebert,H.-C., von der Lieth,C.W., Gilleron,M., Reuter,G., Wittmann, J., Vliegthart, J.F.G. and Gabius, H.-J. (1996b) Carbohydrate-protein interaction. In Gabius,H.-J. and Gabius,S. (eds.), *Glycosciences: Status and Perspectives*. Chapman & Hall, Weinheim, in press.

- Sjoberg,E.R., Manzi,A.E., Khoo,K.H., Dell,A. and Varki,A. (1992) Structural and immunological characterization of *O*-acetylated G<sub>D2</sub>—evidence that G<sub>D2</sub> is an acceptor for ganglioside *O*-acetyltransferase in human melanoma cells. *J. Biol. Chem.*, **267**, 16200–16211.
- Sjoberg,E.R., Powell,L.D., Klein,A. and Varki,A. (1994) Natural ligands of B cell adhesion molecule CD22b can be masked by 9-*O*-acetylation of sialic acids. *J. Cell Biol.*, **126**, 549–562.
- Sun,Y. and Kollman,P.A. (1992) Conformational sampling and ensemble generation by molecular dynamics simulations: 18-Crown-6 as a test case. *J. Comput. Chem.*, **13**, 33–40.
- Thurin,J., Herlyn,M., Hindsgaul,O., Strömberg,N., Karlsson,K.-A., Elder,D., Stepkowski,Z. and Koprowski,H. (1985) Proton NMR and fast-atom bombardment mass spectrometry analysis of the melanoma-associated ganglioside 9-*O*-acetyl G<sub>D3</sub>. *J. Biol. Chem.*, **260**, 14556–14563.
- Varki,A. (1992) Diversity in the sialic acids. *Glycobiology*, **2**, 25–40.
- von der Lieth,C.-W., Schmitz,M., Poppe,L., Hauck,M. and Dabrowski,J. (1989) CARBHYD—ein computergrafisches Interface zur Konstruktion, Wiedergabe und Konformationsberechnung von Poly- und Oligosacchariden. In Gauglitz,G. (ed.), *Software-Entwicklung in der Chemie 3*. Springer Verlag, Heidelberg, pp. 371–378.
- von der Lieth,C.-W., Kozár,T. and Hull,W.E. (1996) A (critical) survey of modeling protocols use to explore the conformational space of oligosaccharides. *J. Mol. Struct. (Theochem)*, in press.
- Zeng,F.-Y. and Gabius,H.-J. (1992) Sialic acid-binding proteins: characterization, biological function and application. *Z. Naturforsch.*, **47c**, 641–653.
- Zeng,F.-Y., Wegenka,U. and Gabius,H.-J. (1992) Purification and properties of a fucoidan-binding protein from human placenta and its identification as immunoglobulin G. *Int. J. Biochem.*, **24**, 1329–1340.
- Zimmer,G., Reuter,G. and Schauer,R. (1992) Use of influenza C virus for detection of 9-*O*-acetylated sialic acids on immobilized glycoconjugates by esterase activity. *Eur. J. Biochem.*, **204**, 209–215.
- Zimmer,G., Suguri,T., Reuter,G., Yu,R.K., Schauer,R. and Herrler,G. (1994) Modification of sialic acids by 9-*O*-acetylation is detected in human leukocytes using the lectin property of influenza C virus. *Glycobiology*, **4**, 343–349.

Received on February 3, 1996; revised on March 23, 1996; accepted on April 24, 1996